 Cytometry 41:9–18 (2000)

# Lymphoma Discrimination by Computerized Triple Matrix Analysis of List Mode Data from Three-Color Flow Cytometric Immunophenotypes of Bone Marrow Aspirates

**R. Bartsch,[1] M. Arland,[2] St. Lange,[2] Ch. Kahl,[1] G. Valet,[3] and H.-G. Höffkes[2]***

[1]Division of Hematology/Oncology, Department of Medicine, Otto-von-Guericke-University of Magdeburg, Germany
[2]Klinikum Fulda, Medizinische Klinik III, Fulda, Germany
[3]Max-Planck-Institute of Biochemistry, Martinsried, Germany

Received 19 November 1999; Revision Received 16 May 2000; Accepted 17 May 2000

**Background:** The goal of this study was to evaluate a self-learning algorithm for the computer classification of information extracted from flow cytometric immunophenotype list mode files from high-grade non-Hodgkin's lymphoma (NHL), Hodgkin's disease (HD), and multiple myeloma (MM).

**Materials and Methods:** Bone marrow aspirates (BMA) were obtained from *untreated* NHL (n = 51), HD (n = 9), or MM (n = 13) patients. Bone marrow aspirates were not infiltrated in NHL and HD patients as confirmed by thorough histologic and cytologic investigation; however, MM patients showed an infiltration rate >50% by malignant myeloma cells. Peripheral blood leukocyte (PBL) samples were taken from age-matched healthy volunteers (n = 44) as easily available control material. A second control group of 15 healthy volunteers, from whom BMA and PBL samples were available, allowed us to differentiate whether the observed classification results on malignant samples were due to the malignant process or simply to the inherent differences between BMA and PBL. Bone marrow aspirates and PBL were analyzed by the same immunophenotyping antibody panel (CD45/14/20, CD4/8/3, kappa/CD19/5, lambda/CD19/5). The acquired list mode data files were analyzed and classified by the self-learning triple matrix classification algorithms CLASSIF1 following a priori separation of the data into a learning set and unknown test set. After completion of the learning phase, known patient samples were reclassified and unknown samples prospectively classified by the algorithm.

**Results:** Highly discriminatory information was extracted for the various lymphoma entities. The most discriminating information was encountered in antibody binding, antibody binding ratios, and relative antibody surface density parameters of leukocytes rather than in percentage frequencies of discrete leukocyte subpopulations. Samples from healthy controls were classified as normal in 97.2% of the cases, whereas those of NHL, HD, and MM patients were on average correctly classified in 80.8% of the cases.

**Conclusions:** Although no detectable lymphoma cells were present in BMA of NHL and HD patients, the CLASSIF1 classification of the immunophenotypes of morphologically normal cells provided a surprisingly good disease discrimination equal or better than that obtained by examining pathological lymph nodes according to the respective literature. The results are suggestive for a lymphoma-related and disease-specific antigen expression shift on normal hematopoietic bone marrow cells that can be used to discriminate the underlying disease (specificity of unspecific changes), i.e., in this case NHL from HD. Multiple myeloma patients were discriminated by changes on malignant as well as on normal bone marrow cells. Cytometry 41:9–18, 2000. © 2000 Wiley-Liss, Inc.

**Key terms:** lymphoma; flow cytometry, list mode; CLASSIF1; data mining

Classification of high-grade/aggressive non-Hodgkin's lymphoma (NHL) is typically based on the analysis of histologic sections, supplemented by immunologic as well as molecular and genetic markers (1). In the past, comparison of pathologic diagnoses has been influenced by the use of different classification systems and, to an even greater extent, by observer-dependent interpretation of the results. The problem is that NHL is heterogeneous in its clinical behavior, morphologic appearance, cellular origin, etiology, and pathogenesis (2).

*Correspondence to: H.-G. Höffkes, Klinikum Fulda, Medizinische Klinik III, Fulda, Germany.
E-mail: hoeffkes.medIII@klinikum-fulda.de

A significant number of studies had the intention to overcome the discrepancies of NHL diagnosis, but the problem of reproducible histopathologic diagnosis (1,3) remains unsolved because no diagnostic feature on its own permits reliable discrimination. Furthermore, a considerable overlap exists between the various diagnostic features in NHL. Until now, molecular diagnosis has not diminished the pathomorphologic pitfalls because a substantial fraction of NHL patients is negative or shows overlaps for major cytogenetic findings.

The goal of this study concerned the discrimination of noninfiltrated bone marrow aspirates (BMA) of NHL and Hodgkin's disease (HD) (<5% blast cells), as well as discrimination of heavily infiltrated multiple myeloma (MM) (>50% malignant cells) BMA against peripheral blood leukocyte (PBL) samples of healthy individuals. Bone marrow aspirates and PBL were immunophenotyped by a four-tube, three-color assay (CD45/14/20, CD4/8/3, kappa/CD19/5, lambda/CD19/5).

Data were analyzed and classified by algorithmic data mining software (4–9) that exhaustively extracts the information from multiparametric flow cytometry list mode files. Lympho-, mono-, and granulocytic cell populations according to their forward (FSC) and sideward (SSC) light scatter characteristics were analyzed in contrast to the usual *selective* lymphocyte analysis. Furthermore antibody binding, antibody binding ratios, and relative surface density of bound antibodies were evaluated in addition to typical percent cell frequency analysis by quadrant analysis of two-parameter fluorescence histograms.

The underlying concept assumes that the exhaustive data analysis of antigen expression on lympho-, mono-, and granulocyte cell populations from *nonoptimal* immunophenotype panels provides sufficient information for the discrimination of several malignant hematopoietic diseases by relying on discriminatory information, not only from malignant but also from normal bystander cells. Normal cells can acquire specific abnormal features as a reaction to the disease process either at the stem cell level (altered differentiation) or by the altered environment (adaptation). This strategy could lead to a significant simplification of immunophenotyping panels provided the vast amount of information can be adequately processed. The concept differs from the usual approach where changes in frequency of directly affected cell populations by standard quadrant analysis of *optimized* immunophenotype panels are investigated. Because only a small fraction (1%–5%) of the available information is evaluated, more and more complex immunophenotype panels are required to gather the necessary amount of discriminatory information. This generates increasing problems of data complexity and consensus formation amongst scientists, whereas the new immunophenotype assay and data analysis concept has the potential of significantly simplifying the discrimination of malignant hematopoietic diseases.

## MATERIALS AND METHODS

### Patient and Sample Characteristics

Age-matched healthy volunteers and patients with NHL, HD, and MM were included in this study after informed consent had been obtained. Diagnostic specimens included anticoagulated (heparin de-novo) BMAs obtained by bone penetration with a Jamshidi needle from the posterior iliac crest by standard technique (10) or PBL samples obtained by venipuncture of the V. cubitalis. Affected lymph nodes of NHL patients exhibited high-grade centroblastic lymphoma according to the Kiel classification and HD patients showed mixed cellularity in affected lymph nodes. The BMA of NHL and HD patients were not infiltrated by lymphoma cells (<5% blast cells) as confirmed by careful pathologic, cytologic, and immunophenotype analysis, whereas BMA from MM patients were heavily infiltrated and contained >50% myeloma cells. The patients were divided into two analysis groups: the learning set containing the BMA samples of 40 NHL, 9 HD, and 13 MM patients as well as the PBL of 36 healthy volunteers; the unknown test set for result verification including BMA samples of 11 NHL patients and PBL of 8 healthy volunteers. The test set samples were a priori selected as patients 1, 5, 10, 15, etc. of the respective patient series. Test samples remained inaccessible during the learning process, i.e., they were *unknown* to the learned classifier.

The concept of the above data collection was to use PBL as a simplified control assay as opposed to BMA controls of healthy volunteers. It had first to be demonstrated that this represents a valid approach. An independent data set of 15 healthy volunteers with BMA and PBL of the same persons was used for this purpose. The antibody panel, assay conditions, instruments setting, data analysis, and learning procedure were identical for both data sets. The comparison between BMA and PBL of healthy volunteers provides a discriminant data pattern for the difference in cellular antigen expression in both body compartments. The prediction is that the use of PBL of healthy volunteers compared to BMA samples of NHL, HD, and/or MM patients shows malignancy-associated changes that are significantly different from the standard BMA/PBL differences of samples from healthy volunteers.

### Immunophenotype Assays

Leukocyte concentrations in peripheral blood and bone marrow samples were adjusted with phosphate-buffered saline (PBS) to $5 \times 10^6$ cells/ml. Monoclonal antibodies (10–20 μl/100 μl diluted blood) were added in pretitered concentrations followed by vortexing and 30-min incubation at 0°C, interrupted by vortexing every 10 min. A quantity of 2 ml Ortho-Lyse (Ortho, Heidelberg, Germany) was subsequently added to the sample with immediate vortexing, followed by 10 min incubation at 0°C for erythrocyte lysis. The sample was washed twice by centrifugation (5 min, 400*g*) with 4 ml PBS, the supernatant was discarded and the sediment resuspended in 2 ml PBS and 0.4 ml PBS/0.5% bovine serum albumin/0.1% Na acide and

kept in the dark on ice until the flow cytometric measurement.

### Antibody Panel

Fluorescein isothiocyanate- (FITC) coupled monoclonal CD45 (T29/33, IgG1 isotype; DAKO Diagnostika, Hamburg, Germany), kappa [rabbit anti-human F(ab′)2, polyclonal; DAKO], lambda (rabbit anti-human F(ab′)2, polyclonal; DAKO], and CD4 (SK3, IgG1 isotype, Becton-Dickinson, Heidelberg, Germany) were used. R-phycoerythrin- (PE) coupled CD8 (SK1, IgG1 isotype, Becton-Dickinson), CD14 (TUEK 4, IgG1 isotype; DAKO), and CD19 (4G7, IgG1 isotype; Becton-Dickinson) were used. Peridinin Chlorophyll A Protein- (PerCP) bound CD3 (SK7, IgG1 isotype, Becton-Dickinson) and CD20 (L27, IgG1 isotype; Becton-Dickinson) were used. Phycoerythrin/Cyanine 5- (PE-Cy5) coupled CD5 (5D7, IgG1 isotype; Caltag Laboratories, San Francisco, CA) was used. The CD45/14/20, CD4/8/3, kappa/CD19/5, and lambda/CD19/5 combinations were analyzed for all samples.

### Flow Cytometry

Cell samples were processed and measured within 2 h after specimen collection. Analysis was performed on a FACScan (Becton-Dickinson) analytical flow cytometer. List mode data were acquired by the Lysis II software (Becton-Dickinson). Fluorescence was excited during the transition of cells through the focal spot of a 15-mW air-cooled argon-ion laser at 488 nm in the sample beam of the flow cytometer. The fluorescence of cell membranes bound to FITC-, PE-, PerCP-, or PE-Cy5-labeled antibodies was determined, as were the cellular FSC and SSC signals.

The instrument set-up was controlled daily with fluorescent reference beads (FCSC, Research Triangle Park, Raleigh-Durham, NC). The instrument set-up for fluorescence intensity and color compensation was monitored in three ways: with lymphocytes from normal persons according to the AUTO-comp software (Becton-Dickinson); with CD4-FITC (SK3; Becton-Dickinson), CD8-PE (SKI; Becton-Dickinson), and CD3-PerCP (SK7; Becton-Dickinson) triple staining of peripheral blood from normal donors selected for erythrocyte or platelet transfusions; and with standardized fluorescent beads (Fluoro Spheres, DAKO).

Fluorescence was collected at 512–547 nm, 572–591 nm, and >610 nm in the FITC, PE, and PerCP/PE-Cy5 fluorescence light channels. Fluorescence compensation was adjusted with hardware circuits. The amplification for FSC and SSC signals was linear, whereas fluorescence signals were amplified by four decade logarithmic amplifiers. All data were collected as FCS 2.0 list mode files and transferred to an IBM personal computer for automated data classification.

### List Mode Analysis

List mode analysis and result classification were performed with the CLASSIF1 program system (Partec, Münster, Germany). Lympho-, mono- and granulocyte gates in the FSC/SSC histogram were automatically set. The logically leading rectangular lymphocyte gate started with predefined border distances to the left and right, as well as to the upper and lower side of the lymphocyte peak (Fig. 1A and 1B). The monocyte gate touched the lymphocyte gate with a total extension on the SSC ordinate of 1.5 times the lymphocyte gate. The granulocyte gate touched the monocyte gate and extended until the high end of the SSC ordinate. The left and right border of the monocyte and granulocyte clusters were set in predefined distances to the respective peaks. The autogating function was capable of correctly gating all list mode files (468 files) of the learning and test set without human interference. The outreach of the left and right borders of the evaluation windows was such that, on average, >95% of all leukocytes were enclosed in the three light-scatter evaluation windows.

The two separation lines determining the quadrants in the FITC/PE, FITC/PerCP, or FITC/PE-Cy5 and the PE/PerCP or PE/PE-Cy5 histograms were fixed for all evaluations at one-third of the fluorescence scale in abscissa and ordinate direction. Fluorescence histograms were evaluated for the FSC/SSC gated lymphocytes, monocytes, and granulocytes separately as three-dimensional cubes (not shown) and two-parameter histograms (Fig. 1C and 1D), i.e., the results of nine two-parameter fluorescence histograms per measurement were available. Seventy-four parameters (6) were extracted for the lymphocyte and similarly for the monocyte and granulocyte cell populations, i.e., 222 parameters for the joint evaluation of all three cell populations per one three-color measurement. A total of $4 \times 222 = 888$ database columns were extracted for each patient with four antibody triplet measurements. Although the analysis concerned lympho-, mono- and granulocytes in PBL, the corresponding BMA samples comprise a very substantial number of cell types (erythroblastic, lymphoblastic, monoblastic and myeloblastic cells, as well as megakaryocytes). Except for CD45-negative erythroblasts, it is not possible to differentiate them properly. In analogy to PBL, they are operatively addressed as lympho-, mono- and granulogate cells based on their FSC/SSC characteristics.

### Data Classification

Expert histopathologic examination of patients' lymph node specimens according to the REAL (1) and Kiel (11) classification served as "clinical truth" for the subsequent learning process. Learning proceeds shortly as follows: The program determines percentile pairs, e.g., 10% and 90% percentiles for the value distribution of the reference samples of each of the database columns. All values of each database column, i.e., from reference and abnormal samples, are subsequently transformed into triple-matrix characters by assignment of 0 to values between the percentiles, + to values above the upper, and − to values below the lower percentile. A triple-matrix replica of the numeric database is available after this data transformation step. The confusion matrix between the known clinical diagnosis of the learning set patients on the ordinate and the computer classification of the cytometrical database

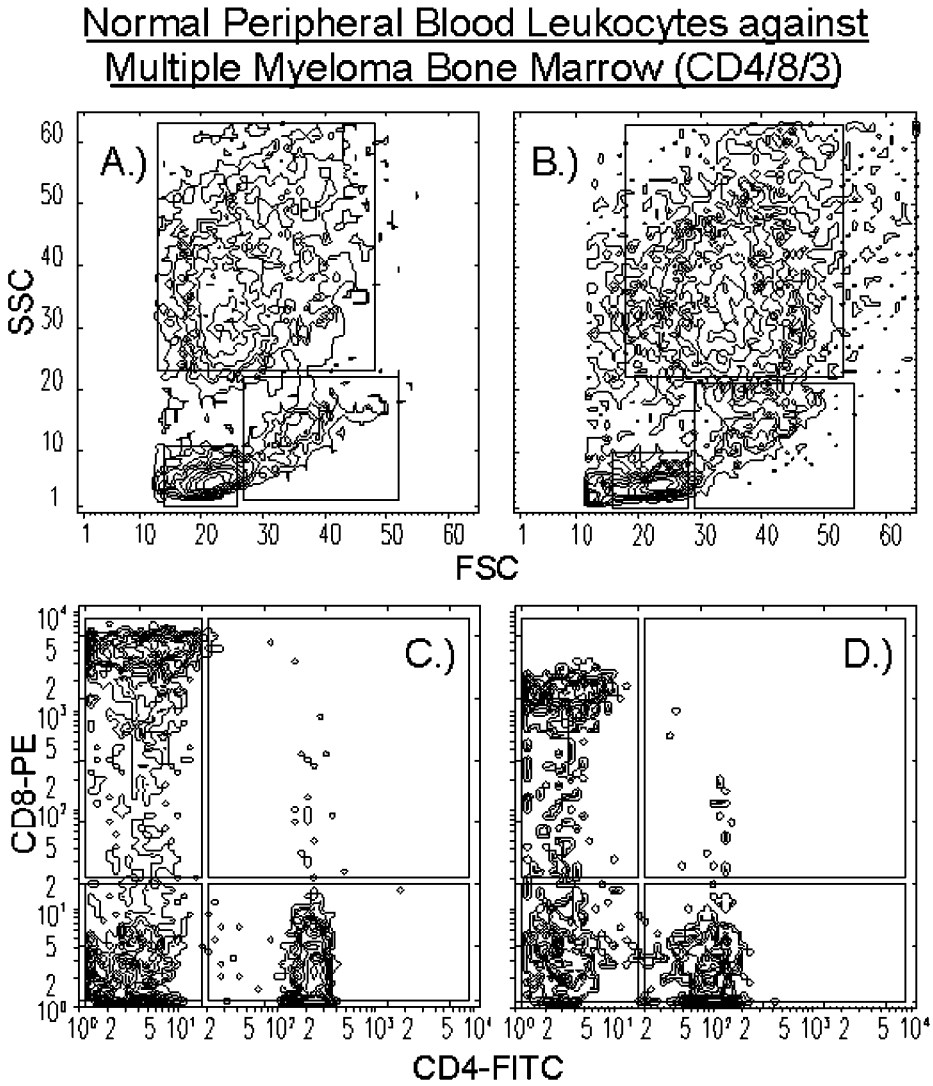


FIG. 1. Automated forward scatter/sidescatter (FSC/SSC)lympho-, mono-, and granulocytic cell population gating of a CD4/8/3 assay for a normal peripheral blood leukocyte (**A**) and a multiple myeloma bone marrow aspirate (**B**) sample at fixed quadrant evaluation windows (**C, D**) at 1/3 of the respective four decade logarithmic flourescence scales. The three decade logarithmic amplitude display, i.e., three contour lines per decade, assures the display of all histogram channels with two and more cells/channel.

parameters on the abscissa is optimized during the subsequent learning process using the triple-matrix database. The values in each diagonal box of the confusion matrix are ideally 100% and 0% in the nondiagonal boxes following correct classification of all patient samples. This is not the case in the beginning of the iterative optimization procedure. The program temporarily removes single database columns or combinations of two database columns in all permutations from consideration, followed each time by a recheck of the classification result. The iteration stops upon completion of all possible combinations. Database columns whose temporary removal either alone or in combination had improved the sum of the diagonal values are then permanently removed.

Following the learning process, each patient sample of the learning set is reclassified according to the highest positional coincidence of its triple matrix with the classifier masks. The quality of the overall classification is judged in a standardized way by the average recognition index (ARI) and the average multiplicity index (AMI). The ARI represents the sum of the diagonal values of the confusion matrix divided by the number of classification states. It should be higher than 80% for clinical purposes. The AMI is a measure for the assignment of more than one classification state to a sample. The AMI is ideally 1.00 in the absence of multiple classifications and 1.1, 1.2, 1.33 when every tenth, fifth, or third example on average is assigned a double classification. Average multiplicity indices of 1.0–1.2 are acceptable in practice. The AMI is calculated as the ratio between the sum of all line sums of the confusion matrix divided by the number of classification states and then by 100. The quality criterion for the

Table 1
*Optimized Discrimination between NHL/HD/MM/PBL Normal (**A**) and BMA Normal/PBL Normal (**B**) using Various Combinations of Lympho-, Mono-, and Granulocytes*[a]

| Cell population | CLASSIF1 classifier | ARI (%) | AMI | Percentiles (%) |
|---|---|---|---|---|
| A. NHL/HD/MM/PBL normal | | | | |
| lym+mon+gran | A7LEARN | 87.9 | 1.05 | 20/80 |
| lym+mon | A8LEARN | 90.5 | 1.04 | 25/75 |
| lym+gran | A9LEARN | 84.9 | 1.01 | 15/85 |
| mon+gran | AALEARN | 89.6 | 1.03 | 20/80 |
| lymphocytes | ABLEARN | 84.2 | 1.07 | 25/75 |
| monocytes | ACLEARN | 80.5 | 1.08 | 15/85 |
| granulocytes | ADLEARN | 79.7 | 1.07 | 20/80 |
| B. BMAnormal/PBL normal | | | | |
| lym+mon+gran | KSLEARN | 96.7 | 1.00 | 10/90 |
| lym+mon | LALEARN | 96.7 | 1.03 | 10/90 |
| lym+gran | LCLEARN | 96.7 | 1.00 | 15/85 |
| mon+gran | LBLEARN | 90.0 | 1.00 | 15/85 |
| lymphocytes | KTLEARN | 93.0 | 1.00 | 15/85 |
| monocytes | KULEARN | 90.0 | 1.00 | 20/80 |
| granulocytes | KVLEARN | 97.3 | 1.00 | 10/90 |

[a]NHL, non-Hodgkin's lymphoma; HD, Hodgkin's disease; PBL, peripheral blood leukocytes; BMA, bone marrow aspirate; lym, lymphocyte; mon, monocyte; gran, granulocyte.

selection of a particular classifier is the highest ARI at the lowest AMI. The classification coincidence factor (CCF) indicates the degree of positional coincidence between the sample classification mask and the classifier masks.

## RESULTS

The list mode data analysis shows the adaptation in the FSC/SSC gates that limit the lympho-, mono- and granulocyte populations in an automated and observer-independent way (Fig. 1A and 1B). It also shows the fixed position of the quadrant analysis windows (Fig. 1C and 1D) for the two-parameter fluorescence histogram projections.

The classification was performed with the joint information of the four antibody triplets for lympho-, mono- and granulogate cell populations either separately or in various combinations (Table 1). This was followed by the separate classification of the results of each antibody triplet jointly for lympho- + mono- + granulogate cells. The discriminatory capacity of the various classifiers was judged by their ARI and AMI values.

All classifications of NHL, HD, and MM patients and healthy volunteers were performed at the 10/90%, 15/85%, 20/80%, 25/75%, and 30/70% percentile pairs. The best discrimination of the NHL/HD/MM/PBL normal data set was achieved for the lympho- + granulogate classifier at the 15/85 percentiles, which identified normal and abnormal samples with 84.9% ARI at 1.01 AMI (Table 1A).

The separate classification of single antibody triplets for lympho-, mono-, and granulocyte cell populations provided less discriminatory results (data not shown), indicating the necessity for the presence of a sufficient amount of relevant classification information for which the information from a single antibody triplet is not sufficient.

The discrimination between BMA and PBL samples both taken from the same person within a separate group of 15 normal individuals provided 96.7% (ARI) correct recognition at 1.00 AMI (Table 1B) for the 15/85 percentile classification; that is, 14 of 15 BMA and 15 of 15 PBL samples were correctly classified. This shows the usefulness of data-pattern classification for an objective BMA quality assessment.

The display of the confusion matrix for the NHL/HD/MM/PBL normal classification (Table 2A**)** indicates positive/negative predictive values of 94.1, 70.0, 91.6/83.3% for the classification. This result is confirmed by the classification of the unknown test set samples (Table 2B) that are similarly classified, i.e., the CLASSIF1 classification is robust towards unknown samples.

The display of the reclassification list (Table 3) of the first 10 samples in each classification category (PBL normal/NHL/HD/MM) shows the differences between the classifier masks (top of rightmost column) as well as among the individual patient classification masks set (lower part of this column). The patient classification masks do not show systematic changes with time as manifested by increasing patients numbers, and the classifications are robust against partial positional noncoincidences between patient classification and the selected classifier mask as indicated by CCFs $<1.00$. Most of the samples are correctly classified although none of them coincides fully with the respective reference classifier mask.

Only 38 data columns (Tables 3 and 4A), i.e., 7.4% of the 512 parameters, were informative for the classification of the clinical patient status and therefore included into the classifier masks. The selected parameters of the classifier masks consisted of 17 lympho- and 21 granulogate parameters. Beside percentage frequency of cells (n = 17), antibody binding (n = 11), antibody binding ratios (n = 7), and relative antibody surface density parameters (n = 1) were selected as discriminatory parameters.

Three of the selected data columns contain the differences between normal BMA and normal PBL, which is represented by the increased presence of CD45-negative erythropoietic cells in BMA. Seven columns contain the discriminatory information between healthy individuals and patients with malignant disease; the remaining 28 columns discriminate among the various malignant diseases. The information for the discrimination between the noninfiltrated BMA (NHL, HD) is located in 14 parameters as opposed to equally 14 parameters for MM patients. The exact relevance of the various discriminatory parameters (Table 4) for the disease processes is not understood at the present time. Nevertheless, a few characteristic features can be described.

Hodgkin's disease is distinguished from NHL mostly by parameters of the CD45/14/20 antibody triplet, whereas the infiltrated MM BMA samples are preferentially discriminated by CD4/8/3, kappa/CD19/5, and lambda/CD19/5 parameters. It is interesting that parameters of granulogate cells constitute a significant part of the selected discrimi-

Table 2
*Discrimination of NHL/HD/MM from Lympho- and Granulocyte Parameters of CD45/14/20, CD4/8/3, k/CD19/5, I/CD19/5 Immunophenotypes*[a]

| Clinical truth | Patients (n) | CLASSIF1 CLASSIFICATION (%) PBL normal | NHL | HD | MM |
|---|---|---|---|---|---|
| A. Learning Set | | | | | |
| PBL normal | 36 | 97.2 | 2.8 | 0.0 | 0.0 |
| NHL | 40 | 15.0 | 80.0 | 7.5 | 0.0 |
| HD | 9 | 0.0 | 11.1 | 77.8 | 11.1 |
| MM | 13 | 15.4 | 0.0 | 0.0 | 84.6 |
| Neg/pos predictive values | | 83.3 | 94.1 | 70.0 | 91.6 |
| B. Unknown Test Set | | | | | |
| Normal | 8 | 100.0 | 0.0 | 0.0 | 0.0 |
| NHL | 11 | 9.1 | 72.7 | 18.2 | 9.1 |

A9LEARN classifier, 15/85% percentiles, ARI = 84.6%, AMI = 1.01.
[a]NHL, non-Hodgkin's lymphoma; HD, Hodgkin's disease; MM, multiple myeloma; PBL, peripheral blood leukocytes.

natory data pattern, indicating that these cells carry information for malignant affections of the lymphatic system. Hodgkin's disease is characterized by an increase of CD45/14-positive granulogate cells, increased CD19 on CD19-negative lymphogate cells, decreased CD19 expression on CD19-positive lymphogate cells, and decreased CD4 and kappa expression. Non-Hodgkin's lymphoma exhibits increased CD14/45 ratios and CD20 on CD45-positive and -negative granulogate cells.

Infiltrated MM BMAs are characterized by decreases of FSC on CD4-negative and CD3-negative, as well as on CD8-positive lymphogate cells. They also are characterized by decreases in the percentage of granulogate cells and of CD19 on CD19neg/5pos as well as on CD19pos/5pos granulogate cells. At the same time, increases of CD14/45 ratios on CD45neg/14pos, of percentage CD45neg/14neg, of percentage CD19pos/5pos, and of percentage CD45neg/20pos granulogate cells are observed.

The classification of the unknown test set (Table 2B) was restricted to normal and NHL samples due to the comparative infrequent availability of HD and MM samples. Bone marrow aspirates from 11 NHL patients without bone marrow infiltration and PBL samples from eight healthy normals were chosen from the initial data set as described in Materials and Methods and classified with the lympho- + granulogate classifier A9LEARN of Table 1. The classification results (Table 2B) show that normal samples were even better recognized (100.0%) than in the learning set (97.2 %, Table 2A). The classification of NHL test set patients (Table 2B) showed a similar overlap with the other classification states as in the learning (Table 2A) at a somewhat reduced recognition rate of 72.7% as opposed to 80.0% for the learning set.

## DISCUSSION

The aim of this study was to explore the discriminatory potential of flow cytometric immunophenotypes of normal cells in the noninfiltrated BMA of NHL and HD patients as opposed to >50% infiltrated BMA of MM patients. This approach was encouraged by the earlier finding that the most discriminatory parameters for NHL classification were not the expert-defined and expected parameters on malignant cells like the relative cell frequencies of lymphogate subpopulations or the light-chain restriction on these cell populations (12,13). Instead, the most discriminatory parameters were total amount of cellular antigen, relative antigen density, and antigen ratio parameters on malignant and normal cells as identified by self-learning computer classification of exhaustively analyzed flow cytometric multicolor immunophenotype list mode data (6).

The requirement for automated classification of multiparametric flow and image cytometry represents an increasingly important challenge. The traditional computer-assisted manual interpretation of flow cytometric histograms is self-limiting due to the inherent complexity of multiparametric data and to the large number of possible permutations in antibody combinations. The advantage of the triple-matrix classification algorithm, used for the analysis of complex immunophenotype results (4–9) consists in the generation of standardized, i.e., interlaboratory, portable classifiers that are robust to the classification of samples from unknown patients.

The selected classification parameters (Table 4) provide an intuitive access to the understanding of the disease discriminating parameters because they consist of a pattern of unmodified database parameters that can be increased (+), decreased (−) or unchanged (0) as compared to the reference patients. No prior knowledge of the data distribution is required and no underlying mathematical assumptions, e.g., on value distribution functions, have to be made for the classification process. The validity of the classification process depends only on representative and clinically well-characterized learning sets, on specificity and quality of the reagents for antigen staining, and on day-to-day intralaboratory measurements precision. The triple-matrix classification approach is therefore not more demanding with respect to the requirements for flow cytometric quality control and standardization than other classification methodologies (14–16).

Table 3
*Reclassification of the Learning Set*

| NR | CLASSIFIER CATEGORIES. | CATEGORY ABBREVIAT | CLASS COINC | CLASSIFIER MASKS |
|---|---|---|---|---|
| 1 | normal | N | 1.00 | 00000000000000000000000000000000000000 |
| 2 | non-Hodgkin lym. | NHL | 1.00 | -+0+0-000--+00-00--00+-++0+-+----+-000 |
| 3 | Hodgkin's lym | HD | 1.00 | -++++-0-0+-+0+-++--0+0-0+-+-+----0-0-- |
| 4 | multiple myeloma | MM | 1.00 | -+0+00-0-00+---++0-+++-0+0-000--+00+-0 |

| NR | RECORD LABELS DATABASE A9LEARN.BI4 | CLASSIF1 CLASSIFI-CATION | CLASS COINC FACT | SAMPLE CLASSIFICATION MASKS = no value |
|---|---|---|---|---|
| 41 | PA0001 N | N | 0.55 | 0+0+000-000.0++000+...00+0+-+-00..-+00 |
| 42 | PA0002 N | N | 0.84 | 00000000000000-0000...00-00+-000..000+ |
| 43 | PA0003 N | N | 0.63 | 0+0+000000000--+0--0..-00+0000--..0000 |
| 44 | PA0004 N | N | 0.76 | +0000+000++.00000000..000+-0000-+00+-0 |
| 45 | PA0006 N | NHL | 0.63 | 0+0+00-00000-0000--+..-++0+-+---+00000 |
| 46 | PA0007 N | N | 0.74 | +0000+-0-00+0-0++00+..0000-0000000000+ |
| 47 | PA0008 N | N | 0.58 | -0+0+-0----.00-0+0+-..0000+0000+..0000 |
| 48 | PA0009 N | N | 0.79 | 0000000+000.0000+000..00+00-+0000+0000 |
| 49 | PA0011 N | N | 0.63 | 0++++0-0-+0.-000000...000+000000..0000 |
| 50 | PA0012 N | N | 0.87 | 00000+00000.0000+0+0..00000000000+0000 |
| 1 | PA0046 NHL | NHL | 0.79 | -+0+0-000-0+0--0+--0..-++00-+----+-+0- |
| 2 | PA0047 NHL | NHL | 0.61 | 0++++0000-00-0-0+--0..-++00-+---00-+0- |
| 3 | PA0048 NHL | NHL | 0.66 | -000000000-+0+-00--0..-0+0++-+0-0+-000 |
| 4 | PA0049 NHL | NHL | 0.66 | -+0+000-000.0+-00--00+-+000000----0000 |
| 5 | PA0051 NHL | NHL | 0.68 | -+0+0--0---.-0-00--0..-++00-+---..0+-0 |
| 6 | PA0052 NHL | N | 0.66 | 0+0+0000000.000++000..-++00000-0..0000 |
| 7 | PA0053 NHL | N | 0.76 | 000000000-0000000-00..-++0000000+0-000 |
| 8 | PA0054 NHL | NHL | 0.63 | 0+0+0000000.00-+0--0..-++0--+---..0+-0 |
| 9 | PA0056 NHL | NHL | 0.66 | 0+0+0000000+00-00-00..-0000-+---..+000 |
| 10 | PA0057 NHL | N | 0.61 | -++++-0-00-.0--+0++0..0+0+000000000000 |
| 77 | PA0096 HD | HD | 0.61 | -++++-+000-++00+000-..00+-+-+----+-00- |
| 78 | PA0097 HD | HD | 0.53 | -++++-+0++-++00++00.0+00+-+-+-00--0000 |
| 79 | PA0098 HD | HD | 0.68 | -++++-0-00-.0+0++00...000-+-+---..-0-- |
| 80 | PA0099 HD | HD | 0.71 | -++++-0-0--+0+-00--+00-++-+-+0--..---0 |
| 81 | PA0101 HD | HD | 0.68 | -++++------.---++--...-++-+-+---..-0-- |
| 82 | PA0102 HD | NHL | 0.61 | 0+0+0-0-0--+0+-+0--++0-+00+000--+00-00 |
| 83 | PA0103 HD | MM | 0.50 | -+0+0----0-.-+-+0--0+0-+00+00+-0..0-0+ |
| 84 | PA0104 HD | HD | 0.68 | -++++-000+-.000++000..00++0-+---00-0-- |
| 85 | PA0106 HD | HD | 0.66 | -+0+0-000+-+-0-++--0..-0+-0000--..-0-- |
| 86 | PA0107 MM | MM | 0.58 | 0+0+0000000+0+-++0-0..-000+000-0..-0-- |
| 87 | PA0109 MM | N | 0.66 | 0+0+00-0000.--000000..-00+0-+0-0+00000 |
| 88 | PA0110 MM | MM | 0.68 | -+0+00-0--00---++--+..-000--+---0+0+-- |
| 89 | PA0111 MM | MM | 0.68 | -+0+0000000+0--000-0..0000-000--..0+-0 |
| 90 | PA0112 MM | MM | 0.66 | 0+0+00-0--00---++000..000+-000--..0+00 |
| 91 | PA0114 MM | MM | 0.66 | 0+0+00-0-00+-+-++000..00++0000-0..0+00 |
| 92 | PA0115 MM | MM | 0.55 | -+0+0--0---+-+-++0--..-00-++-+-0..0--0 |
| 93 | PA0116 MM | MM | 0.66 | -+0+0--0---+-+-++0-00+00+00000--..-000 |
| 94 | PA0117 MM | N | 0.63 | 0+0+000-00000+-00--+0+-+-0-+-+-0+0+-00 |
| 95 | PA0119 MM | MM | 0.74 | -++++0---00+---+0--++0-++0-000--0+-+-0 |

The reduction of the classification parameters to the most informative parameters avoids the problem of statistically overdetermined learning sets. The number of 888 (lympo-, mono- and granulocyte), 512 (lympho- granulocyte, lympho- monocyte, mono- granulocyte) or 222 (lymphocyte, monocyte, granulocyte) database columns as classification parameters in the initial data set (Table 1) is substantially higher than the number of patients in the different groups, but the number of finally selected parameters (n = 38/19) (Tables 3, 4A, and 4B) is substan-

Table 4
*Parameter Pattern of the Lymphocyte/Granulocyte NHL/HD/MM/PBL Normal Classification with Four Three-Color Assays*[a]

| Classification mask parameter | Cell parameter | Parameter changes | | | |
|---|---|---|---|---|---|
| | | PBL | NHL | HD | MM |
| A. BMAnormal/PBL normal Discrimination | | | | | |
| 1 | % lympho (CD45/14/20 assay, BMA/PBL par#3) | 0 | − | − | − |
| 2 | % CD45neg in lymphogate (BMA/PBL par#1) | 0 | + | + | + |
| 4 | % CD45neg/CD14neg in lymphogate (BMA/PBL par#2) | 0 | + | + | + |
| B. Malignancy indicators | | | | | |
| 15 | CD19 on CD19pos/CD5neg lymphogate | 0 | − | − | − |
| 19 | CD45 rel.surf.dens on CD45pos granulogate | 0 | − | − | − |
| 23 | CD45 on CD45pos/CD14neg granulogate | 0 | − | − | − |
| 31 | CD14 on CD14neg/CD20neg granulogate | 0 | − | − | − |
| 32 | % CD14pos/CD20neg in granulogate | 0 | − | − | − |
| 12 | % CD45neg/CD20pos in lymphogate | 0 | + | + | + |
| 25 | CD8/CD4 ratio on CD4pos/CD8neg in granulogate | 0 | + | + | + |
| C. Malignancy discriminators NHL/HD | | | | | |
| 3 | % CD14pos in lymphogate | 0 | 0 | + | 0 |
| 5 | % CD45pos/CD14pos in lymphogate | 0 | 0 | + | 0 |
| 14 | CD19 on CD19neg/CD5pos in lymphogate | 0 | 0 | + | − |
| 16 | CD5/CD19 ratio on CD19pos/CD5neg in lymphogate | 0 | 0 | + | + |
| 17 | CD5/lambda ratio on lambda pos/CD5neg in lymphogate | 0 | 0 | + | + |
| 21 | CD45 on CD45neg/CD14pos in granulogate | 0 | 0 | + | + |
| 8 | CD4 on CD4pos in lymphogate | 0 | 0 | − | 0 |
| 26 | kappa rel.surf.dens on kappa pos in granulogate | 0 | 0 | − | 0 |
| 37 | CD19 on CD19pos/CD5pos in granulogate | 0 | 0 | − | − |
| 38 | CD5/lambda ratio on lambneg/CD5pos in granulogate | 0 | 0 | − | 0 |
| 22 | CD14/CD45 ratio on CD45neg/CD14pos in granulogate | 0 | + | 0 | + |
| 24 | CD14/CD45 ratio on CD45pos/CD14neg in granulogate | 0 | + | 0 | 0 |
| 34 | CD20 on CD45neg/CD20pos in granulogate | 0 | + | 0 | 0 |
| 10 | CD8/CD4 ratio on CD4pos/CD8pos in lymphogate | 0 | − | + | 0 |
| D. MM | | | | | |
| 7 | FSC CD4neg in lymphogate | 0 | 0 | 0 | − |
| 9 | FSC CD8pos in lymphogate | 0 | 0 | 0 | − |
| 13 | FSC CD3neg in lymphogate | 0 | 0 | 0 | − |
| 20 | % CD45neg/CD14neg in granulogate | 0 | 0 | 0 | + |
| 36 | % CD19pos/CD5pos in granulogate | 0 | 0 | 0 | + |
| 6 | % lymphogate cells (CD8/4/3 assay) | 0 | − | − | 0 |
| 11 | % lympho kappa/CD19/5 in lymphogate | 0 | − | − | 0 |
| 18 | CD45 on CD45pos in granulogate | 0 | − | − | 0 |
| 28 | % lambda neg in granulogate | 0 | − | − | 0 |
| 30 | % lambda neg/CD19neg in granulogate | 0 | − | − | 0 |
| 35 | CD3 on CD8neg/CD3pos in granulogate | 0 | − | − | 0 |
| 33 | % CD45neg/CD20pos in granulogate | 0 | − | − | + |
| 27 | % granulogate cells | 0 | + | + | − |
| 29 | % lambda pos in granulogate | 0 | + | + | 0 |

[a]A9LEARN classifier, 15/85% percentiles, 38 of 512 available lympho- and granulogate cell parameters (7.4%) contain the discriminatory information. The triple matrix characters in the last column represent the classifier masks of Table 3 (top of the rightmost column of reclassification list). The parameters of the table are realigned in comparison to Table 3 according to malignancy indicator and malignancy discriminator parameters. NHL, non-Hodgkin's lymphoma; HD, Hodgkin's disease; MM, multiple myeloma; PBL, peripheral blood leukocytes.

tially lower than the number of patients (n = 98), i.e., the classification matrix is not overdetermined in a statistical sense. An important quality criterion for computer classification consists of the correct classification of unknown test samples. CLASSIF1 classifiers have proven to be quite robust in this respect (4, 6, 8).

The successful classification of the learning set (Table 2A) and the very substantial difference between the BMA/PBL discriminatory parameter pattern of normal individuals (Table 5) and the NHL/HD/MM parameter pattern (Table 4) including the selection of 57.8% (Table 4) and 52.6% (Table 5) of antigen expression parameters indicates a definitive antigen shift of nonmalignant bone marrow cells in NHL and HD patients. This antigen shift is different between NHL and HD patients. Only three parameters of the normal BMA/PBL discrim-

Table 5
*Parameter Pattern for Lymphocyte+Granulocyte Classification of BMAnormal/PBLnormal with Four Three-Color Assays*[a]

| Classification mask parameter | Cell parameter | Param changes PBL | BMA |
|---|---|---|---|
| 1 | % CD45neg in lymphogate (NHL/HD/MM par#2) | 0 | + |
| 2 | % CD45neg/CD14neg in lymphogate (NHL/HD/MM par#4) | 0 | + |
| 3 | % lymphogate cells (CD45/14/20 assay, NHL/HD/MM par#1) | 0 | − |
| 4 | % kappa pos/CD19neg in lymphogate | 0 | + |
| 5 | % CD8neg/CD3neg in lymphogate | 0 | + |
| 6 | % kappa neg/CD5neg in lymphogate | 0 | + |
| 7 | % CD5neg in lymphogate | 0 | + |
| 8 | % CD19pos/CD5neg in lymphogate | 0 | + |
| 9 | % lambda neg/CD5neg in lymphogate | 0 | + |
| 10 | CD14 on CD14pos cells in granulogate | 0 | − |
| 11 | CD14 on CD45pos/CD14pos cells in granulogate | 0 | − |
| 12 | CD8 on CD8pos in granulogate | 0 | − |
| 13 | CD19 on CD19pos in granulogate | 0 | − |
| 14 | CD19 on lambda pos/CD19pos in granulogate | 0 | − |
| 15 | CD14 on CD14pos/CD20pos cells in granulogate | 0 | − |
| 16 | CD45 on CD45pos/CD20pos in granulogate | 0 | − |
| 17 | CD3/CD8 ratio on CD8pos/CD3neg in granulogate | 0 | + |
| 18 | CD5/kappa ratio on kappa pos/CD5pos in granulogate | 0 | − |
| 19 | CD5/lambda ratio on lambda pos/CD5pos in granulogate | 0 | − |

[a]LCLEARN classifier, 15/85% percentiles, 19 of 512 available lympho- and granulocyte parameters (3.7%) contain the discriminatory information. BMA, bone marrow aspirate; PBL, peripheral blood leukocyte.

inatory data pattern (Table 5) are found among the 38 parameters of the NHL/HD/BM classifier data pattern (Table 4), clearly indicating that the observed discrimination of the malignant patients is not based on the inherent difference between normal BMA and normal PBL cells. This is a further example of the earlier observation (6) that BMA samples can be classified against PBL controls, which represents a significant simplification for BMA immunophenotype classification in routine clinical practice.

It is unclear at present whether the antigen shift of normal BMA cells in NHL and HD patients represents an altered cell differentiation in the presence or as cause of the malignant process or whether it is induced by adaptive changes of normally differentiated cells. This observation may permit the detection of NHL or HD from PBL instead of BMA samples. It seems also reasonable to assume that list mode files from lymph node specimens are suitable in the same manner for computerized classification. A new approach for the diagnosis of hematologic disorders in lymph nodes by standardized cytometry may arise from such considerations.

It is surprising that so much information for discrimination between NHL, HD, and MM is provided by an immunophenotype panel that is normally not designed for this purpose. If the concept of not optimally adapted immunophenotype panels together with exhaustive data analysis and classification can be generalized, it will not only be possible to simplify complex immunophenotype panels but also to collect a significant amount of information on changes and altered reactivity of nonmalignant bystander cells as response or as cause of the malignant processes, as well as on the relevant behavior of the various cell populations during chemotherapy or irradiation.

It is in any case clear that the present CLASSIF1 classification of information from normal BMA cells provides an equal or better discrimination between NHL and HD (Table 2) than the one achieved by histologic examination of the affected lymph nodes, where typical recognition rates of 46%–86% have been published (17,18).

## LITERATURE CITED

1. Harris NL, Jaffe ES, Stein H. A revised European-American classification of lymphoid neoplasms: a proposal from the international lymphoma study group. Blood 1994;84:1361–1392.
2. Brittinger G, Bartels H, Common H, Duhmke E, Fulle H, Gunzer U, Gyenes T, Heinz R, König E, Meusers P, Paukstat M, Pralle H, Stein H, Feller AC, Lennert K. Clinical and prognostic relevance of the Kiel classification of non-Hodgkin's lymphomas: Results of a prospective multicenter study by the Kiel Lymphoma Study group. Hematol Oncol 1984;2:269–306.
3. Thews O, Thews A, Huber Ch, Vaupel P. Computer-assisted interpretation of flow cytometry data in hematology. Cytometry 1996;23: 140–149.
4. Valet G, Kahle H, Otto F, Bräutigam E, Kestens L. Prediction and precise diagnosis of diseases by data pattern analysis in multiparameter flow cytometry: melanoma, juvenile asthma, HIV infection. In: Darzynkiewicz Z, Robinson JP, Crissman HA, editors. Cytometry, 3rd edition. San Diego: Academic Press, 2000; in press.
5. Valet G, Roth G, Kellermann W. Risk assessment for intensive care patients by automated classification of flow cytometric oxidative burst, serine and cysteine proteinase activity measurements using classif1 triple matrix analysis. In: Robinson JP, Babcock G, editors. Cytometric cellular analysis. New York: Wiley-Liss, Inc; 1998. pp 289–306.
6. Valet G K, Höffkes H-G. Automated classification of patients with chronic lymphocytic leukemia and immunocytoma from flow cytometric three-color immunophenotypes. Cytometry 1997;30: 275–288.
7. Tarnok A, Hambsch J, Borte M, Valet G, Schneider P. Immunological and serological discrimination of children with and without postsur-

gical capillary leak syndrome. In: Faist E, editor. The immune consequences of trauma, shock and sepsis. Bologna: Monduzzi; 1997. pp 845–849.
8. Valet G, Valet M, Tschöpe D, Gabriel H, Rothe G, Kellermann W, Kahle H. White cell and thrombocyte disorders: standardized, self-learning flow cytometric list mode data classification with the classif1 program system. Ann NY Acad Sci 1993;677:233–251.
9. Gabriel H, Valet G, Urhausen A, Kindermann W. Selbstlernende Klassifizierung durchflußzytometrischer Listendaten von immunphänotypisierten Lymphozyten bei akuter körperlicher Arbeit. Dtsch Z Sportmed 1993;44:461–465.
10. Jamshidi K, Swaim WR. Bone marrow biopsy with unaltered architecture. A new biopsy device. J Lab Clin Med 1974;77:335–342.
11. Lennert K, Mohri N, Stein H, Kaiserling E. The histopathology of malignant lymphoma. Br J Haematol 1975;31:193–203.
12. Terstappen LWM, Mickaels RA, Dost R, Loken MR. Increased light scattering resolution facilitates multidimensional flow cytometric analysis. Cytometry 1990;11:506–512.
13. Leary JF. Strategies for rare cell detection and isolation. Methods Cell Biol 1994;42:331–358.
14. Decaestecker Ch, Remmelink M, Salmon I, Camby I, Goldschmidt D, Patein M, Van Ham Ph, Pasteels JL, Kiss R. Methodological aspects of using decision trees to characterize Leiomyomatous tumors. Cytometry 1996;24:83–92.
15. Diamond LW, Nguyen DT, Andreeff M, Maiese RL, Braylan RC. A knowledge-based system for the interpretation of flow cytometric data in leukemia and lymphomas. Cytometry 1994;17:266–273.
16. Frankel DS, Frankel SL, Binder BJ, Vogt RF. Application of neural networks to flow cytometry data analysis and real-time cell classification. Cytometry 1996;23:290–302.
17. Sheibani K, Nathwani BN, Swartz WG, Ben-Ezra J, Brownell MD, Burke JS, Kennedy JL, Koo CH, Winberg CD. Variability in interpretation of immunohistologic findings in lymphoproliferative disorders by hematopathologists. A comprehensive statistical analysis of interobserver performance. Cancer 1988;62:657–664.
18. NCI Non-Hodgkin's Classification Project Writing Committee. Classification of non-Hodgkin's lymphomas. Reproducibility of major classification systems. Cancer 1985;55:91–95.